Published in final edited form as:
Circ Res. 2010 October 15; 107(8): 1002–1010. doi:10.1161/CIRCRESAHA.110.217018.

Local Regulation of Arterial L-Type Calcium Channels by Reactive Oxygen Species

Gregory C. Amberg, Ph.D, **Scott Earley, Ph.D**, and **Stephanie A. Glapa**
Vascular Physiology Research Group, Department of Biomedical Sciences, Colorado State University, Fort Collins, CO 80523

Abstract

Rationale—Reactive oxygen species (ROS) are implicated in the development of cardiovascular disease and oxidants are important signaling molecules in many cell types. Recent evidence suggests that localized subcellular compartmentalization of ROS generation is an important feature of ROS signaling. However, mechanisms that transduce localized subcellular changes in redox status to functionally-relevant changes in cellular processes such as Ca^{2+} influx are poorly understood.

Objective—To test the hypothesis that ROS regulate L-type Ca^{2+} channel activity in cerebral arterial smooth muscle.

Methods and Results—Using a TIRF (total internal reflection fluorescence) imaging-based approach, we found that highly-localized subplasmalemmal generation of endogenous ROS preceded and colocalized with sites of enhanced L-type Ca^{2+} channel sparklet activity in isolated cerebral arterial smooth muscle cells. Consistent with this observation and our hypothesis, exogenous ROS increased localized L-type Ca^{2+} channel sparklet activity in isolated arterial myocytes via activation of protein kinase C alpha (PKCα) and when applied to intact cerebral arterial segments, exogenous ROS increased arterial tone in an L-type Ca^{2+} channel-dependent fashion. Furthermore, angiotensin II-dependent stimulation of local L-type Ca^{2+} channel sparklet activity in isolated cells and contraction of intact arteries was abolished following inhibition of NADPH oxidase.

Conclusions—Our data support a novel model of local oxidative regulation of Ca^{2+} influx where vasoconstrictors coupled to NAPDH oxidase (e.g., angiotensin II) induce discrete sites of ROS generation resulting in oxidative activation of adjacent PKCα molecules that in turn promote local sites of enhanced L-type Ca^{2+} channel activity resulting in increased Ca^{2+} influx and contraction.

Keywords

reactive oxygen species; L-type calcium channels; calcium sparklets; protein kinase C

Introduction

Oxidative and reductive biochemical processes are integral components of cellular biology. However, disruption of cellular redox status beyond physiological parameters is correlated with disorders ranging from cardiovascular disease to neurodegeneration to cancer. The

Corresponding Author: Gregory C. Amberg, Ph.D, Colorado State University, Department of Biomedical Sciences, 1617 Campus Delivery, Fort Collins, CO 80523, Phone: 970-491-6028, Fax: 970-491-7907, Gregory.Amberg@colostate.edu.

Disclosures
None.

cardiovascular system appears to be particularly sensitive to perturbations in redox balance with increased oxidative stress implicated in the development of cardiovascular diseases including heart failure, atherosclerosis, stroke and hypertension 1–5. The apparent sensitivity of the cardiovascular system to redox imbalance may reside in the relative functional importance of redox signaling under physiological conditions. Redox biochemistry has been studied extensively in the vasculature 4, 6–9 with specialized subcellular compartmentalization, regulation, and generation of reactive oxygen species (ROS) emerging a common theme 10–12. However, mechanisms that transduce localized subcellular changes in redox signaling to functionally-relevant changes in cellular processes such as Ca^{2+} influx are less clear.

Peripheral arterial resistance is determined by the contractile state of arterial smooth muscle which is tightly coupled to Ca^{2+} influx through L–type voltage-dependent Cav1.2 Ca^{2+} channels 13–15. Total internal reflection fluorescence (TIRF) microscopy has been used to image L-type Ca^{2+} channel (Ca^{2+} sparklet) activity in arterial smooth muscle cells with high temporal and spatial resolution 16–19. Using this approach, a high-activity mode of Cav1.2 Ca^{2+} channel function was identified. These studies revealed that high-activity Ca^{2+} sparklets resulted from spatially restricted enhancement of Cav1.2 Ca^{2+} channel function by protein kinase C alpha (PKCα). PKCα-dependent Ca^{2+} sparklet activity was found to be necessary for normal arterial function 16, 19, 20. In addition, increased PKCα-dependent Ca^{2+} sparklet activity was associated with altered gene expression and arterial dysfunction in experimental models of hypertension 19, 20. Despite these intriguing observations, the molecular mechanisms underlying high-activity localized PKCα-dependent L-type Ca^{2+} channel function are poorly understood.

Using a novel TIRF imaging-based approach, we identified and characterized a mechanism that functionally links local oxidant signaling to sustained colocalized L-type Ca^{2+} channel activity. We demonstrate for the first time that highly-localized subplasmalemmal generation of endogenous ROS precede and colocalize with enhanced L-type Ca^{2+} channel activity in cerebral arterial smooth muscle. Consistent with this observation, ROS increased L-type Ca^{2+} channel sparklet activity via activation of PKCα and increased arterial tone in an L-type Ca^{2+} channel-dependent fashion. Taken together, our data suggest that local oxidative activation of PKCα-dependent L-type Ca^{2+} influx represents a functionally relevant convergence of oxidant and Ca^{2+} signaling pathways in cerebral arterial smooth muscle with physiological and pathological implications.

Methods

Male Sprague-Dawley rats were euthanized with sodium pentobarbital (200 mg/kg intraperitoneally) as approved by the Institutional Animal Care and Use Committee of Colorado State University. Smooth muscle cells were isolated from basilar and cerebral arteries.

Arteries for intact tissue experiments were cannulated, pressurized with bicarbonate-based physiological saline solution, and superfused with aerated physiological saline solution at 37°C. To block the effects of endothelial-derived nitric oxide, we used the nitric oxide synthase inhibitor N^G-nitro-L-arginine (L-NNA; 300 μmol/L). Intravascular pressure was maintained at 80 mmHg and inner diameter was continuously monitored.

We used the conventional whole-cell patch-clamp technique to voltage clamp freshly isolated arterial myocytes. L-type Ca^{2+} channel sparklets were recorded with a through-the-lens TIRF system with 60X (numerical aperture = 1.49) and 100X (numerical aperture = 1.45) TIRF oil-immersion objectives. All TIRF experiments were performed in the presence

of thapsigargin (1 μmol/L). To monitor Ca^{2+} influx, myocytes were loaded with the Ca^{2+} indicator fluo-5F (200 μmol/L) via dialysis through the patch pipette. L-type Ca^{2+} channel sparklets were visualized and recorded at a holding potential of −70 mV with elevated external [Ca^{2+}] (20 mmol/L) to facilitate the detection of Ca^{2+} sparklet events and provide fluorescent signals of sufficient amplitude 17 to permit quantal analysis of Ca^{2+} sparklet activity. Fluo-5F fluorescence was converted to [Ca^{2+}] and analyzed as previously reported using a custom automated algorithm 17, 21. Ca^{2+} sparklet activity was quantified 17, 18 by calculating the nP_s of each sparklet site, where n is the number of quantal levels, and P_s is the probability that a given Ca^{2+} sparklet site is active. As with previous reports 17, 18, Ca^{2+} sparklet activity was bimodally distributed with sites of low activity (nP_s 0 to 0.2) and high activity (nP_s>0.2). TIRF microscopy was also used to visualize subplasmalemmal ROS generation in isolated arterial myocytes using the cell-permeant ROS indicator 5-(and-6)-chloromethyl-2′7′-dichlorodihydrofluorescein diacetate acetyl ester (DCF; 10 μmol/L).

For our immunofluorescence studies we used a mouse monoclonal PKCα antibody (Abcam) with an Alexa Fluor 488-conjugated rabbit anti-mouse secondary antibody on freshly prepared myocytes. Fluorescence was undetectable in control experiments where either the primary or the secondary antibody was omitted (data not shown). Membrane and cytosolic PKCα-associated fluorescence was quantified by measuring the intensity of pixels above a set threshold. We determined the ratio of plasma membrane to cytosolic PKCα-associated fluorescence and used this as an indicator of PKCα translocation and activity 19, 22.

Normally distributed data are presented as the mean ± standard error of the mean (SEM) with comparisons performed using parametric tests. For bimodally distributed Ca^{2+} sparklet activity (i.e. nP_s) datasets comparisons were performed using non-parametric tests. Arithmetic means of nP_s datasets are indicated in the figures (solid red horizontal lines) for non-statistical purposes. *P* values less than 0.05 were considered significant and asterisks (*) in the figures indicate a significant difference between groups.

An expanded Materials and Methods section can be found in the online data supplement at http://circres.ahajournals.org.

Results

To test the overall hypothesis that ROS regulate L-type Ca^{2+} channel activity in cerebral arterial smooth muscle we formulated four specific requisite criteria: 1) Exogenous ROS should increase arterial tone in a L-type Ca^{2+} channel-dependent manner; 2) exogenous ROS should stimulate Ca^{2+} sparklet activity in isolated myocytes; 3) inhibition of endogenous ROS generation should limit arterial contraction and prevent stimulation of Ca^{2+} sparklet activity; and 4) endogenous ROS production should colocalize with Ca^{2+} sparklet activity.

Exogenous ROS increase arterial tone in pressurized cerebral arteries

We examined the effects of ROS on arterial smooth muscle function by exposing pressurized cerebral arteries (80 mmHg at 37°C) to the ROS generating system xanthine oxidase (XO; 0.2 mU/mL) plus hypoxanthine (HX; 250 μmol/L; Figure 1). The nitric oxide synthase inhibitor L-NNA (300 μmol/L) was present to preclude contractile responses from ROS-dependent reductions in nitric oxide 23. Following the development of a stable level of myogenic tone (24.8±2.5 %, n=8 arteries), we exposed arteries to HX followed by XO/HX and monitored changes in luminal diameter. While HX alone had no effect (*P*>0.05, n=8 arteries), addition of XO reversibly reduced luminal diameter by 18.1±6.9 μm corresponding to a 10.7±4.1 % increase in arterial tone (Figure 1A and B; *P*<0.05, n=8 arteries). Transient dilations were occasionally observed (in 3 out of 8 arteries) following addition of XO. In the

presence of the L-type Ca^{2+} channel antagonist diltiazem (10 μmol/L), which nearly abolished arterial tone (from 23.6±7.1 % to 4.4±1.7 %), XO/HX was without effect (Figure 1C and D; $P>0.05$, n=3 arteries). Although multiple mechanisms are certainly involved in arterial contractile responses to XO/HX, these data are consistent with the hypothesis that ROS increase arterial tone by stimulating L-type Ca^{2+} channel function.

Exogenous ROS stimulate L-type Ca^{2+} channel sparklet activity in isolated cerebral arterial smooth muscle cells

To test the hypothesis that ROS stimulate L-type Ca^{2+} channel activity, we recorded Ca^{2+} sparklets in isolated voltage-clamped (−70 mV) arterial myocytes before and after XO/HX (2 mU/mL/250 μmol/L). As shown in Figure 2A, XO/HX exposure increased Ca^{2+} sparklet activity. To further characterize the effects of ROS on Ca^{2+} sparklets we constructed Ca^{2+} sparklet amplitude histograms under control conditions and after XO/HX (Figure 2B). Fitting these distributions with a multi-component Gaussian function revealed that Ca^{2+} sparklet amplitudes were quantal and that stimulation by ROS increased the number of quanta activated but not the amplitude of the quantal event (34 nmol/L [Ca^{2+}] for control and 36 nmol/L [Ca^{2+}] for XO/HX). Note that the Ca^{2+} sparklet quantal amplitudes before and after XO/HX approximate those previously reported for arterial smooth muscle L-type Ca^{2+} channels and for heterologously expressed Cav1.2 L-type Ca^{2+} channels 17, 18, 20, 24. From these data we conclude that ROS increase Ca^{2+} influx by stimulating localized L-type Ca^{2+} channel activity.

Next we quantified L-type Ca^{2+} channel activity by determining the nP_s of each Ca^{2+} sparklet site, where n is the number of quantal levels detected and P_s is the probability that a given Ca^{2+} sparklet site is active. As evident in the histogram in Figure 2B, Ca^{2+} sparklet activity (nP_s) increased after XO/HX exposure with the number of high-activity Ca^{2+} sparklet sites ($nP_s \geq 2$) increasing from 2 to 16 (Figure 2C; $P<0.05$, n=8 cells). In addition to increasing Ca^{2+} sparklet activity, XO/HX also increased Ca^{2+} sparklet site density ≈3.5-fold by promoting Ca^{2+} influx at regions previously devoid of activity (Figure 2D; $P<0.05$, n=8 cells). These data suggest that ROS stimulate localized L-type Ca^{2+} channel function by increasing the occurrence of high-activity Ca^{2+} sparklet sites and by stimulating nascent Ca^{2+} sparklet activity.

Stimulation of L-type Ca^{2+} channel sparklet activity by exogenous ROS is PKCα-dependent

PKCα, which is subject to oxidative activation 25, stimulates L-type Ca^{2+} channel sparklet activity 17, 18. Accordingly, we tested the effects of XO/HX on PKCα activation in arterial myocytes with immunofluorescence by using the level of plasma membrane-associated PKCα as an indicator of activation 19, 22 (Figure 3A). Under control conditions (HX; 250 μmol/L), PKCα-associated fluorescence was diffusely cytosolic with few discrete elevations along the plasma membrane. In contrast, following XO/HX exposure (2 mU/mL/250 μmol/L), and indicative of activation, PKCα-associated fluorescence was characterized by prominent focal elevations near (≤1 μm) the plasma membrane (Figure 3B; $P<0.05$, n=15 cells).

Our PKCα immunofluorescence data suggest that ROS could increase L-type Ca^{2+} channel sparklet activity by activating PKCα. To examine this possibility, we tested the effects of XO/HX on Ca^{2+} sparklets in the presence of the PKC inhibitor Gö6976 (100 nmol/L). In contrast to experiments in the absence of Gö6976 (e.g., Figure 2), XO/HX had no effect on Ca^{2+} sparklet activity or density following inhibition of PKCα (Figure 3C and D; $P>0.05$, n=5 cells). These data suggest that ROS stimulate L-type Ca^{2+} channel sparklet activity via activation of PKCα.

NADPH oxidase inhibition prevents Ang II-dependent stimulation of L-type Ca^{2+} channels and arterial constriction

Ang II stimulates ROS-generating NADPH oxidase signaling complexes. Therefore, we used Ang II to examine the role of endogenous ROS generation on Ca^{2+} sparklet activity and arterial constriction. As shown previously 19, 20, Ang II (100 nmol/L) increased L-type Ca^{2+} channel sparklet activity (nP_s) and the number of active Ca^{2+} sparklet sites (Figure 4A and B; $P<0.05$, n=8 cells). This effect was blocked by the AT1 receptor antagonist ZD7155 (500 nmol/L; control $nP_s=0.35\pm0.32$, Ang II + ZD7155 $nP_s=0.30\pm0.11$, $P>0.05$, n=4 cells). Inhibition of NADPH oxidase-mediated ROS generation with apocynin (25 μmol/L) 9 abolished the effect of Ang II on Ca^{2+} sparklet activity and density (Figure 4C and D; $P>0.05$, n=6 cells). Unlike PKC inhibition with Gö6976, apocynin prevented stimulation of Ca^{2+} sparklets by Ang II but had no effect on Ca^{2+} sparklet sites previously active under control conditions ($P>0.05$, n=5 cells). This indicates that the effects of apocynin are not the result of PKC inhibition or by direct blockade of L-type Ca^{2+} channels as suggested for other NADPH oxidase inhibitors (e.g. diphenyleneiodonium 26). Note that Ang II and apocynin (and XO/HX) produced similar results in conventional recordings of macroscopic arterial L-type Ca^{2+} currents (see Online Supplement Figure I).

Ang II produces endothelium-independent arterial constriction via stimulation of AT1 receptors 27, 28 (also see Figure 5A). Similar to our Ca^{2+} sparklet experiments, inhibition of NADPH oxidase with apocynin (and PKC with Gö6976) abolished contractile responses to Ang II (1 nmol/L; Figure 5B, C and D; $P<0.05$, n=3 arteries). Taken together, these data support our hypothesis that generation of endogenous ROS is necessary for AT1-dependent Ang II stimulation of L-type Ca^{2+} channels and arterial constriction.

Ang II stimulates L-type Ca^{2+} channel sparklet activity via local production of ROS

If generation of endogenous ROS is necessary for Ang II-dependent stimulation of L-type Ca^{2+} channels, then sites of Ca^{2+} sparklet activity should colocalize with endogenous sites of ROS production. We used TIRF microscopy to visualize subplasmalemmal generation of ROS in response to Ang II. Isolated myocytes were loaded with the ROS indicator DCF (10 μmol/L). Figure 6A shows TIRF images of DCF fluorescence under control conditions and after application Ang II (100 nmol/L; both in Ca^{2+}-free buffer). Interestingly, discrete sites (puncta) of elevated DCF fluorescence were apparent under control conditions (0.006 ± 0.002 puncta per μm^2) and increased in number ≈3.5-fold with Ang II (0.021 ± 0.002 puncta per μm^2; $P<0.05$; n=6 cells). The amplitude of the DCF elevations before and after Ang II were not different ($P<0.05$; n=6 cells). Ca^{2+} sparklet site and ROS puncta densities (0.025 ± 0.005 and 0.021 ± 0.002, respectively) were similar ($P>0.05$).

Having demonstrated that increased ROS production (as with Ca^{2+} sparklet activity) in response to Ang II is localized, we developed an experimental approach to visualize the spatial distributions of ROS generation (with DCF) and L-type Ca^{2+} channel sparklet activity (with fluo-5F) in the same cell. First, we loaded isolated myocytes with DCF in Ca^{2+} free buffer (as above), placed a patch pipette on the cell, formed a GΩ seal (i.e., established the cell-attached patch configuration), and applied Ang II (100 nmol/L). Upon visualization of sites of punctate elevations in DCF fluorescence (Figure 7A, panel 1, time course i), negative pressure was applied to the interior of the pipette to rupture the plasma membrane (i.e., establish the whole-cell patch configuration) thus dialyzing the cell with fluo-5F. Next, we replaced the Ca^{2+}-free external solution with one containing 20 mmol/L Ca^{2+} and monitored for Ca^{2+} sparklet activity. Strikingly, we found that the sites of ROS generation colocalized with high-activity ($nP_s=0.56\pm0.26$) Ca^{2+} sparklet sites (Figure 7A, panel 2, time course ii; n=6 sites from 5 cells). While Ca^{2+} sparklet sites were always associated with a preceding site of ROS generation, we did observe three sites of ROS

generation that were not associated with subsequent Ca^{2+} sparklet activity (data not shown; n=3 ROS sites in 7 cells).

To further establish the proximity of punctate ROS generation and Ca^{2+} sparklet activity we thresholded (mean basal fluo-5F fluorescence plus three times its standard deviation) our fluo-5F fluorescence images to isolate Ca^{2+} sparklet fluorescence and merged them (Figure 7A, panel 3) with the DCF images (Figure 7A, panel 1). As evident in the composite image (Figure 7A, panel 4), sites of punctate ROS generation and Ca^{2+} sparklet activity were closely apposed. Indeed, the average distance between the peaks of ROS puncta and Ca^{2+} sparklet sites was less than 1 μm (0.91±0.24 μm; n=6 sites from 5 cells). To place this distance into perspective, the average cell area imaged during these experiments was 99.2±13.7 μm^2 and the probability, by chance alone, that we would observe 6 ROS puncta and 6 Ca^{2+} sparklet sites ≈1 μm apart in this area is less than 1 in 1,000,000 (see Detailed Methods in the Online Supplement for details). From these data we conclude that sites of ROS generation precede and colocalize with sites of L-type Ca^{2+} channel sparklet activity.

Discussion

In this study we combined TIRF imaging with conventional techniques to test the hypothesis that ROS regulate L-type Ca^{2+} channel activity in cerebral arterial smooth muscle. The major findings in support of this hypothesis are: 1) Exogenous ROS generated by xanthine oxidase constrict pressurized cerebral arteries in an L-type Ca^{2+} channel-dependent manner; 2) exogenous ROS increase PKCα-dependent L-type Ca^{2+} channel sparklet activity in isolated arterial myocytes; 3) generation of endogenous ROS by NADPH oxidase is necessary for stimulation of Ca^{2+} sparklets and contraction by Ang II; and 4) Ang II induces localized sites of ROS production that precede and colocalize with subsequent Ca^{2+} sparklet activity. These observations support a model (see Figure 7D) of local oxidative regulation of Ca^{2+} influx where vasoconstrictors coupled to NAPDH oxidase (e.g., Ang II) induce discrete sites of ROS generation resulting in activation of adjacent PKCα molecules. PKCα activation in turn promotes localized L-type Ca^{2+} channel (i.e., sparklet) activity resulting in increased Ca^{2+} influx and arterial contraction. To the best of our knowledge, our model provides the first experimentally-based mechanistic framework whereby local changes in redox signaling result in changes in Ca^{2+} influx and arterial function.

ROS impairment of endothelial function leads to increased arterial tone 23, 29. Our observation that XO/HX constricts cerebral arteries (presumably via PKC activation) after endothelial nitric oxide synthase inhibition with L-NNA suggests that ROS also increase tone through smooth muscle-specific mechanisms. Activation of arterial smooth muscle PKC by ROS could induce contraction by a minimum of four non-mutually exclusive mechanisms: 1) Increased localized L-type Ca^{2+} channel sparklet activity as characterized here; 2) modulation of other plasmalemmal ion channels (e.g., inhibition of hyperpolarizing potassium channels 30 or activation of depolarizing transient receptor potential channels 31); 3) decreased hyperpolarizing ryanodine receptor-dependent Ca^{2+} spark activity 32; and 4) sensitization of the arterial smooth muscle contractile apparatus to Ca^{2+} 33. The discrete subcellular nature of Ang II-dependent ROS generation demonstrated here suggests that the relationship between ROS and these diverse regulatory mechanisms could be determined in part by coincident localization of ROS generating and smooth muscle regulatory signaling complexes. In addition, differential subcellular distributions of signaling complexes and ROS generating enzymes could account for contradictory data regarding the effect of ROS on arterial tone (i.e., contraction 34 versus relaxation 35).

PKC stimulation of NADPH oxidase is well-documented 36, 37. However, reciprocal activation of PKC by ROS in arterial smooth muscle, as shown here, has not been reported.

Oxidative activation of PKCα leads to sustained cofactor-independent kinase activity 25, 38. Sustained PKC activity is consistent with the observation that established high-activity L-type Ca^{2+} channel sparklet sites are abolished by PKC inhibition 17. Application of exogenous ROS did not produce a uniform translocation of PKCα to the plasma membrane. Rather, accumulation of PKCα at the plasma membrane was irregular with punctate elevations in PKCα-associated fluorescence (Figure 3). Similarly, the increase in Ca^{2+} sparklet site density by exogenous ROS was far less than predicted if ROS exposure resulted in a generalized non-specific translocation of PKC to the plasma membrane. Importantly, previous work in arterial smooth muscle cells has shown that the scaffold protein AKAP150 is necessary for punctate membrane localization of PKCα and Ca^{2+} sparklet activity 19. In this context, our observation that ROS exposure produced spatially restricted PKCα-dependent Ca^{2+} sparklet activity suggests that while ROS may induce PKC activation, additional components such as AKAP150 are necessary for efficient targeting of the kinase to the plasma membrane to stimulate localized L-type Ca^{2+} channel activity.

Our imaging of punctate sites of endogenous ROS generation in isolated cells with DCF indicates that stimulation of L-type Ca^{2+} channels by ROS would also be restricted by the localized nature of ROS production and not just by limited membrane targeting of PKCα *per se*. However, PKC phosphorylation of p47phox is an important step in the initial activation of NADPH oxidase by Ang II 9, 39. Thus, PKC regulation of L-type Ca^{2+} channels likely involves (at least) two events where PKC first stimulates the production of NADPH oxidase-derived ROS which in turn oxidatively activates PKCα resulting in enhanced Ca^{2+} sparklet activity. Our data do not address this hypothesis directly. However, during our ROS imaging experiments the external solution was free of Ca^{2+} and we incubated the cells with the sarcoplasmic reticulum Ca^{2+}-ATPase inhibitor thapsigargin. Thus, neither Ca^{2+} entry into the cell or release from of Ca^{2+} from internal stores appear to be necessary for ROS generation in response to Ang II in isolated arterial myocytes.

In combination with supporting data, our sequential ROS/Ca^{2+} imaging experiments provide compelling evidence suggesting that endogenous ROS locally regulate L-type Ca^{2+} channel activity. Using this unique approach we found that ROS production preceded and colocalized with sites of L-type Ca^{2+} channel sparklet activity (respective peaks less than 1 μm apart). It is possible that the molecular components necessary for ROS production and L-type Ca^{2+} channel activity share the same subcellular location but are independent and not functionally linked. However, our data showing that: 1) Exogenous ROS promote PKCα activation and translocation to the plasma membrane; 2) exogenous ROS stimulate PKC-dependent Ca^{2+} sparklet activity and; 3) inhibition of endogenous ROS generation with apocynin abolished stimulation of Ca^{2+} sparklets by Ang II renders this possibility unlikely. Note that whether apocynin is acting as a *bone fide* inhibitor of NADPH oxidase or as an antioxidant 40 does not contradict our overall hypothesis that localized generation of ROS stimulate L-type Ca^{2+} channel activity.

To conclude, in this study we provide compelling evidence in support of the hypothesis that local changes in redox status are transduced to sustained Ca^{2+} influx through L-type Ca^{2+} channels (i.e. high-activity Ca^{2+} sparklets). The implications and questions raised by our observations are intriguing. What molecular components are necessary for the formation of this novel signalosome? Are other signaling pathways subject to or influenced by similar local regulation by ROS? Does localized oxidative activation of L-type Ca^{2+} channels contribute to enhanced Ca^{2+} influx during hypertension? The data presented here may provide a mechanistic starting point for future efforts aimed at answering these important questions.

Novelty and Significance

What Is Known?

- Reactive oxygen species (ROS) are important signaling molecules in cardiovascular cells.
- Because of their reactive nature and as a mechanism conferring specificity, ROS production is thought to be localized in order for them to function effectively.
- Highly localized L-type calcium channel activity has been observed in arterial smooth muscle cells and shown to contribute to arterial contraction.

What New Information Does This Article Contribute?

- Exogenous ROS increase localized protein kinase C-dependent L-type calcium channel activity in isolated arterial smooth muscle cells and constrict intact arteries in an L-type calcium channel-dependent manner.
- Generation of endogenous ROS by NADPH oxidase is necessary for stimulation of L-type calcium channels and arterial contraction in response to the vasoconstrictor angiotensin II.
- Angiotensin II induces punctate sites of ROS generation that precede and colocalize with L-type calcium channel activity in isolated arterial smooth muscle cells.

Summary

ROS and calcium are essential components of arterial function under physiological and pathophysiological conditions. However, the relationship between these two signaling modalities is unclear. In this study we investigated the functional and spatial relationship between ROS and L-type calcium channels, a major source of cytoplasmic calcium in arterial smooth muscle. We found that ROS stimulated local sites of L-type calcium channel activity in isolated arterial smooth muscle cells and induced contraction of intact arterial segments. Using a novel imaging-based approach, we visualized punctate sites of endogenous ROS formation in isolated arterial smooth muscle cells. We also show, for the first time, that the spatial distribution of these ROS puncta overlaps with that of local L-type calcium channel activity. These observations indicate that discrete sites of ROS generation are functionally and spatially coupled to local calcium influx through single L-type calcium channels in arterial smooth muscle cells. ROS are widely implicated in the pathogenesis of hypertension. As the relationship between ROS and L-type calcium channels results in increased channel function, our findings should provide mechanistic insight into events underlying increased calcium influx during hypertension and lead to the development of new rational therapies for managing and preventing disease.

Supplementary Material

Refer to Web version on PubMed Central for supplementary material.

Acknowledgments

We thank Dr. Michael Tamkun for critically reading this manuscript.

Sources of Funding

This work as supported by the American Heart Association (0635118N to G.C.A.; 0535226N to S.E.), the Colorado State University College Research Council (to G.C.A.), the Pew Scholars Program (to G.C.A), and the National Institutes of Health (R01HL091905 to S.E.).

Non-standard Abbreviations and Acronyms

Ang II	angiotensin II
DCF	5-(and-6)-chloromethyl-2′7′-dichlorodihydrofluorescein diacetate acetyl ester, HX, hypoxanthine
L-NNA	N^G-nitro-L-arginine
PKCα	protein kinase C alpha
ROS	reactive oxygen species
TIRF	total internal reflection fluorescence
XO	xanthine oxidase

References

1. Adiga IK, Nair RR. Multiple signaling pathways coordinately mediate reactive oxygen species dependent cardiomyocyte hypertrophy. Cell Biochem Funct. 2008; 26:346–351. [PubMed: 18283710]
2. Allen CL, Bayraktutan U. Oxidative stress and its role in the pathogenesis of ischaemic stroke. Int J Stroke. 2009; 4:461–470. [PubMed: 19930058]
3. Hordijk PL. Regulation of NADPH oxidases: The role of Rac proteins. Circ Res. 2006; 98:453–462. [PubMed: 16514078]
4. Lee MY, Griendling KK. Redox signaling, vascular function, and hypertension. Antioxid Redox Signal. 2008; 10:1045–1059. [PubMed: 18321201]
5. Paravicini TM, Touyz RM. NADPH oxidases, reactive oxygen species, and hypertension: Clinical implications and therapeutic possibilities. Diabetes Care. 2008; 31 (Suppl 2):S170–180. [PubMed: 18227481]
6. Ambasta RK, Kumar P, Griendling KK, Schmidt HH, Busse R, Brandes RP. Direct interaction of the novel Nox proteins with p22phox is required for the formation of a functionally active NADPH oxidase. J Biol Chem. 2004; 279:45935–45941. [PubMed: 15322091]
7. Garrido AM, Griendling KK. NADPH oxidases and angiotensin II receptor signaling. Mol Cell Endocrinol. 2008
8. Quinn MT, Ammons MC, Deleo FR. The expanding role of NADPH oxidases in health and disease: No longer just agents of death and destruction. Clin Sci (Lond). 2006; 111:1–20. [PubMed: 16764554]
9. Touyz RM, Chen X, Tabet F, Yao G, He G, Quinn MT, Pagano PJ, Schiffrin EL. Expression of a functionally active gp91phox-containing neutrophil-type NAD(P)H oxidase in smooth muscle cells from human resistance arteries: Regulation by angiotensin II. Circ Res. 2002; 90:1205–1213. [PubMed: 12065324]
10. Brown DI, Griendling KK. Nox proteins in signal transduction. Free Radical Biology and Medicine. 2009; 47:1239–1253. [PubMed: 19628035]
11. Helmcke I, Heumüller S, Tikkanen R, Schröder K, Brandes RP. Identification of structural elements in Nox1 and Nox4 controlling localization and activity. Antioxidants & Redox Signaling. 2009; 11:1279–1287. [PubMed: 19061439]
12. Hilenski LL, Clempus RE, Quinn MT, Lambeth JD, Griendling KK. Distinct subcellular localizations of Nox1 and Nox4 in vascular smooth muscle cells. Arterioscler Thromb Vasc Biol. 2004; 24:677–683. [PubMed: 14670934]

13. Knot HJ, Nelson MT. Regulation of arterial diameter and wall [Ca^{2+}] in cerebral arteries of rat by membrane potential and intravascular pressure. J Physiol. 1998; 508 (Pt 1):199–209. [PubMed: 9490839]
14. Moosmang S, Schulla V, Welling A, Feil R, Feil S, Wegener JW, Hofmann F, Klugbauer N. Dominant role of smooth muscle L-type calcium channel Cav1.2 for blood pressure regulation. EMBO J. 2003; 22:6027–6034. [PubMed: 14609949]
15. Rubart M, Patlak JB, Nelson MT. Ca^{2+} currents in cerebral artery smooth muscle cells of rat at physiological Ca^{2+} concentrations. J Gen Physiol. 1996; 107:459–472. [PubMed: 8722560]
16. Amberg GC, Navedo MF, Nieves-Cintron M, Molkentin JD, Santana LF. Calcium sparklets regulate local and global calcium in murine arterial smooth muscle. J Physiol. 2007; 579:187–201. [PubMed: 17158168]
17. Navedo MF, Amberg GC, Nieves M, Molkentin JD, Santana LF. Mechanisms underlying heterogeneous Ca^{2+} sparklet activity in arterial smooth muscle. J Gen Physiol. 2006; 127:611–622. [PubMed: 16702354]
18. Navedo MF, Amberg GC, Votaw VS, Santana LF. Constitutively active L-type Ca^{2+} channels. Proc Natl Acad Sci U S A. 2005; 102:11112–11117. [PubMed: 16040810]
19. Navedo MF, Nieves-Cintron M, Amberg GC, Yuan C, Votaw VS, Lederer WJ, McKnight GS, Santana LF. AKAP150 is required for stuttering persistent Ca^{2+} sparklets and angiotensin II-induced hypertension. Circ Res. 2008; 102:e1–e11. [PubMed: 18174462]
20. Nieves-Cintron M, Amberg GC, Navedo MF, Molkentin JD, Santana LF. The control of Ca^{2+} influx and NFATc3 signaling in arterial smooth muscle during hypertension. Proc Natl Acad Sci U S A. 2008; 105:15623–15628. [PubMed: 18832165]
21. Maravall M, Mainen ZF, Sabatini BL, Svoboda K. Estimating intracellular calcium concentrations and buffering without wavelength ratioing. Biophys J. 2000; 78:2655–2667. [PubMed: 10777761]
22. Khalil RA, Lajoie C, Morgan KG. In situ determination of $[Ca^{2+}]_i$ threshold for translocation of the alpha-protein kinase C isoform. Am J Physiol. 1994; 266:C1544–1551. [PubMed: 8023886]
23. Schulz E, Jansen T, Wenzel P, Daiber A, Münzel T. Nitric oxide, tetrahydrobiopterin, oxidative stress, and endothelial dysfunction in hypertension. Antioxidants & Redox Signaling. 2008; 10:1115–1126. [PubMed: 18321209]
24. Navedo MF, Amberg GC, Westenbroek RE, Sinnegger-Brauns MJ, Catterall WA, Striessnig J, Santana LF. $Ca_V1.3$ channels produce persistent calcium sparklets, but $Ca_V1.2$ channels are responsible for sparklets in mouse arterial smooth muscle. Am J Physiol Heart Circ Physiol. 2007; 293:H1359–1370. [PubMed: 17526649]
25. Gopalakrishna R, Anderson WB. Ca^{2+}- and phospholipid-independent activation of protein kinase C by selective oxidative modification of the regulatory domain. Proc Natl Acad Sci U S A. 1989; 86:6758–6762. [PubMed: 2505261]
26. Weir EK, Wyatt CN, Reeve HL, Huang J, Archer SL, Peers C. Diphenyleneiodonium inhibits both potassium and calcium currents in isolated pulmonary artery smooth muscle cells. J Appl Physiol. 1994; 76:2611–2615. [PubMed: 7928890]
27. Touyz RM, Schiffrin EL. Signal transduction mechanisms mediating the physiological and pathophysiological actions of angiotensin II in vascular smooth muscle cells. Pharmacol Rev. 2000; 52:639–672. [PubMed: 11121512]
28. Wackenfors A, Vikman P, Nilsson E, Edvinsson L, Malmsjo M. Angiotensin II-induced vasodilatation in cerebral arteries is mediated by endothelium-derived hyperpolarising factor. Eur J Pharmacol. 2006; 531:259–263. [PubMed: 16410000]
29. Rubanyi GM, Vanhoutte PM. Superoxide anions and hyperoxia inactivate endothelium-derived relaxing factor. Am J Physiol Heart Circ Physiol. 1986; 250:H822–827.
30. Rainbow RD, Norman RI, Everitt DE, Brignell JL, Davies NW, Standen NB. Endothelin-1 and angiotensin II inhibit arterial voltage-gated K^+ channels through different protein kinase C isoenzymes. Cardiovasc Res. 2009; 83:493–500. [PubMed: 19429666]
31. Earley S, Straub SV, Brayden JE. Protein kinase C regulates vascular myogenic tone through activation of TRPM4. Am J Physiol Heart Circ Physiol. 2007; 292:H2613–2622. [PubMed: 17293488]

32. Bonev AD, Jaggar JH, Rubart M, Nelson MT. Activators of protein kinase C decrease Ca^{2+} spark frequency in smooth muscle cells from cerebral arteries. Am J Physiol Cell Physiol. 1997; 273:C2090–2095.
33. Kitazawa T, Takizawa N, Ikebe M, Eto M. Reconstitution of protein kinase C-induced contractile Ca^{2+} sensitization in triton X-100-demembranated rabbit arterial smooth muscle. J Physiol. 1999; 520(Pt 1):139–152. [PubMed: 10517807]
34. Tabet F, Savoia C, Schiffrin EL, Touyz RM. Differential calcium regulation by hydrogen peroxide and superoxide in vascular smooth muscle cells from spontaneously hypertensive rats. J Cardiovasc Pharmacol. 2004; 44:200–208. [PubMed: 15243301]
35. Miller AA, Drummond GR, Schmidt HH, Sobey CG. NADPH oxidase activity and function are profoundly greater in cerebral versus systemic arteries. Circ Res. 2005; 97:1055–1062. [PubMed: 16210546]
36. Cox JA, Jeng AY, Sharkey NA, Blumberg PM, Tauber AI. Activation of the human neutrophil nicotinamide adenine dinucleotide phosphate (NADPH)-oxidase by protein kinase C. J Clin Invest. 1985; 76:1932–1938. [PubMed: 2997297]
37. Ungvari Z, Csiszar A, Huang A, Kaminski PM, Wolin MS, Koller A. High pressure induces superoxide production in isolated arteries via protein kinase C-dependent activation of NAD(P)H oxidase. Circulation. 2003; 108:1253–1258. [PubMed: 12874194]
38. Knapp LT, Klann E. Superoxide-induced stimulation of protein kinase C via thiol modification and modulation of zinc content. J Biol Chem. 2000; 275:24136–24145. [PubMed: 10823825]
39. Seshiah PN, Weber DS, Rocic P, Valppu L, Taniyama Y, Griendling KK. Angiotensin II stimulation of NAD(P)H oxidase activity: Upstream mediators. Circ Res. 2002; 91:406–413. [PubMed: 12215489]
40. Heumuller S, Wind S, Barbosa-Sicard E, Schmidt HH, Busse R, Schroder K, Brandes RP. Apocynin is not an inhibitor of vascular NADPH oxidases but an antioxidant. Hypertension. 2008; 51:211–217. [PubMed: 18086956]

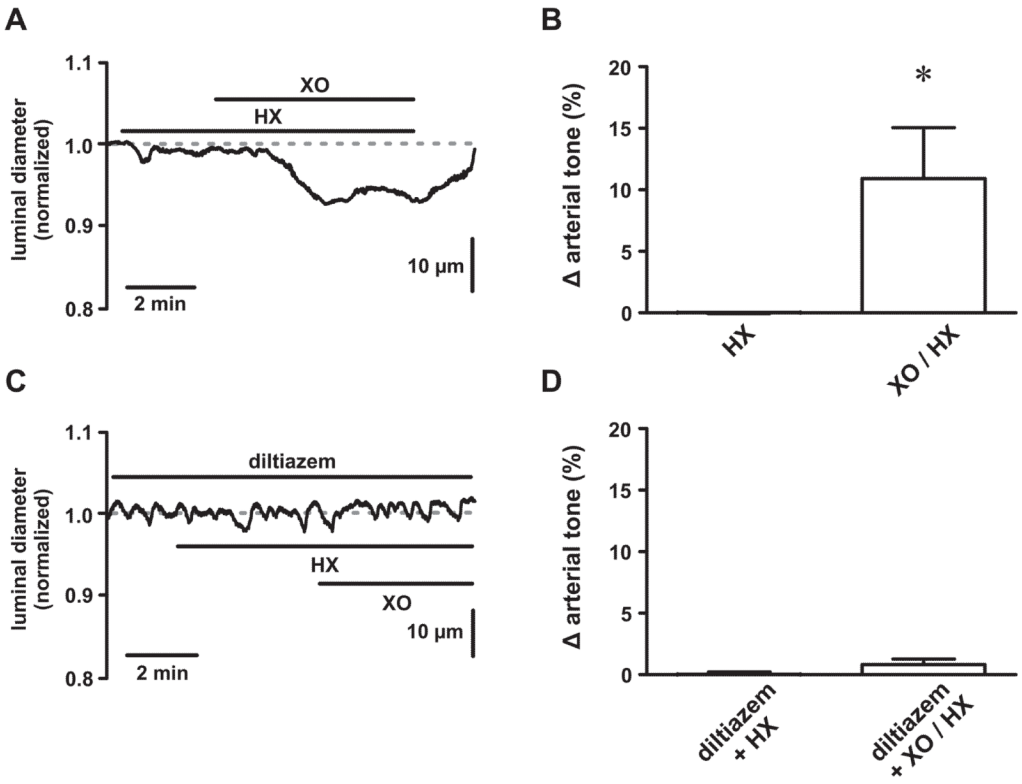

Figure 1. Reactive oxygen species increase tone in pressurized cerebral arteries

A, Representative time course showing the luminal diameter of a pressurized (80 mm Hg) cerebral artery exposed to hypoxanthine (HX; 250 μmol/L) followed by xanthine oxidase (XO; 0.2mU/mL) plus HX. B, Plot of the mean ± SEM change in arterial tone (% Δ arterial tone) during HX and XO/HX exposure (n=7 arteries). C, Representative time course showing the luminal diameter of a pressurized (80 mm Hg) cerebral artery exposed to HX followed by XO/HX in the presence of the L-type Ca^{2+} channel blocker diltiazem (10 μmol/L). D, Plot of the mean ± SEM change in arterial tone (% Δ arterial tone) during diltiazem + HX and diltiazem + XO/HX exposure (n=3 arteries). **P*<0.05

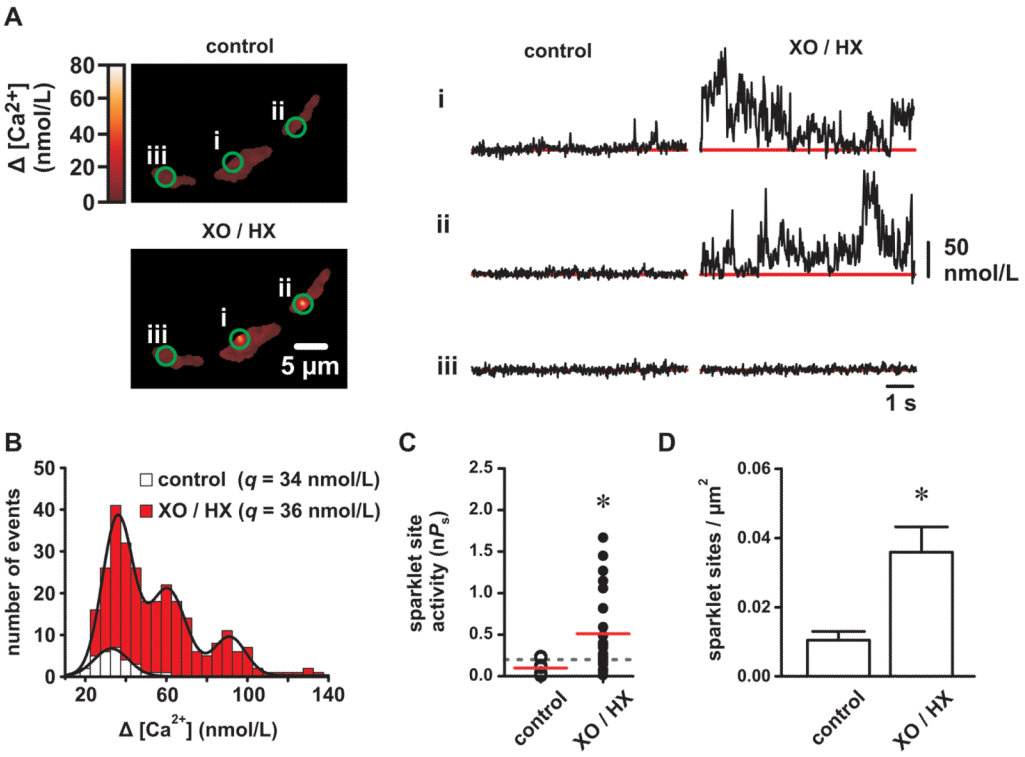

Figure 2. Reactive oxygen species increase L-type Ca^{2+} channel sparklet activity in isolated cerebral arterial smooth muscle cells

A, Representative TIRF images showing Ca^{2+} influx in an arterial myocyte before and after application of XO and HX (2mU/mL and 250 μmol/L, respectively). Traces show the time course of Ca^{2+} influx at the three circled sites before and after XO/HX. B, Ca^{2+} sparklet amplitude histograms before (white) and after XO/HX exposure (red). The solid black lines are best-fits to the control (q=34 nmol/L) and to the XO/HX (q=36 nmol/L) histograms with a multi-component Gaussian function where q is the quantal unit of Ca^{2+} influx (see Detailed Methods in the Online Supplement). C, Plot of Ca^{2+} sparklet site activities (nP_s) before and after XO/HX (n=8 cells). The red solid lines are the arithmetic means of each group and the dashed line marks the threshold for high-activity Ca^{2+} sparklet sites ($nP_s \geq 0.2$). D, Plot of the mean ± SEM Ca^{2+} sparklet density (Ca^{2+} sparklet sites/μm^2) before and after XO/HX (n=8 cells). *P<0.05

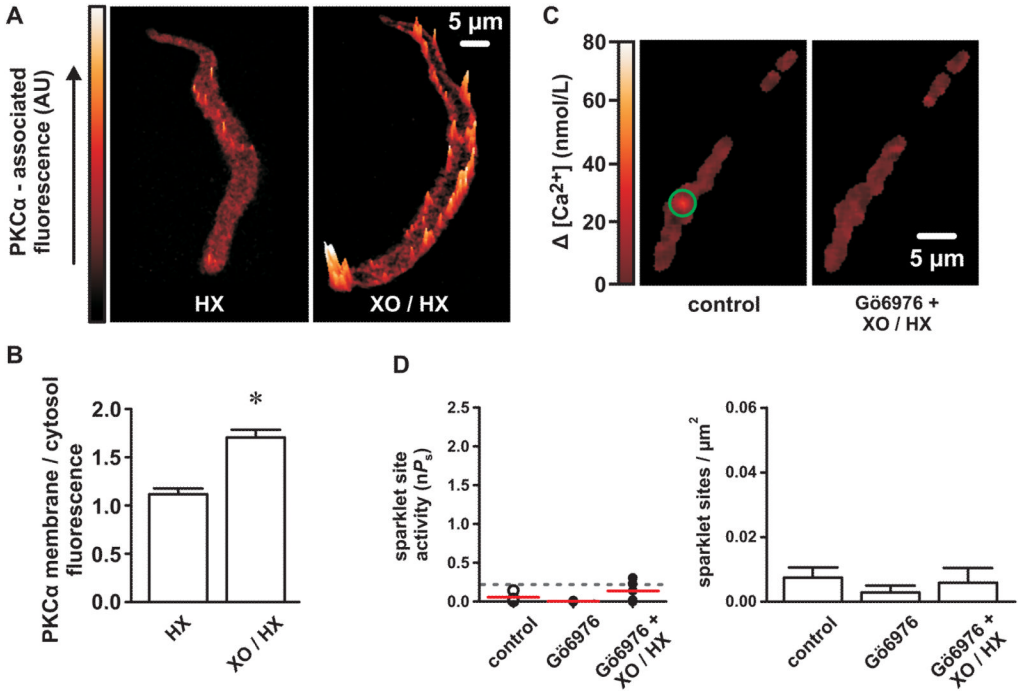

Figure 3. Reactive oxygen species increase L-type Ca^{2+} channel sparklet activity via stimulation of PKC

A, Representative surface plots of PKCα-associated immunofluorescence in cerebral arterial myocytes exposed to either HX alone (250 μmol/L) or XO and HX (2 mU/mL and 250 μmol/L, respectively). B, Bar plot of the mean ± SEM membrane-to-cytosol PKCα-associated fluorescence ratios in HX- and XO/HX-exposed myocytes (n=15 cells from three independent experiments). C, Representative TIRF images showing Ca^{2+} influx in an arterial myocyte under control conditions and after exposure to XO and HX (2 mU/mL and 250 μmol/L, respectively) in the presence of the PKC inhibitor Gö6976 (100 nmol/L). D, Plot of Ca^{2+} sparklet site activities (nP_s) and mean ± SEM Ca^{2+} sparklet density (Ca^{2+} sparklet sites/μm^2) under control conditions and after exposure to XO and HX in the presence of Gö6976 (n=5 cells). *P<0.05

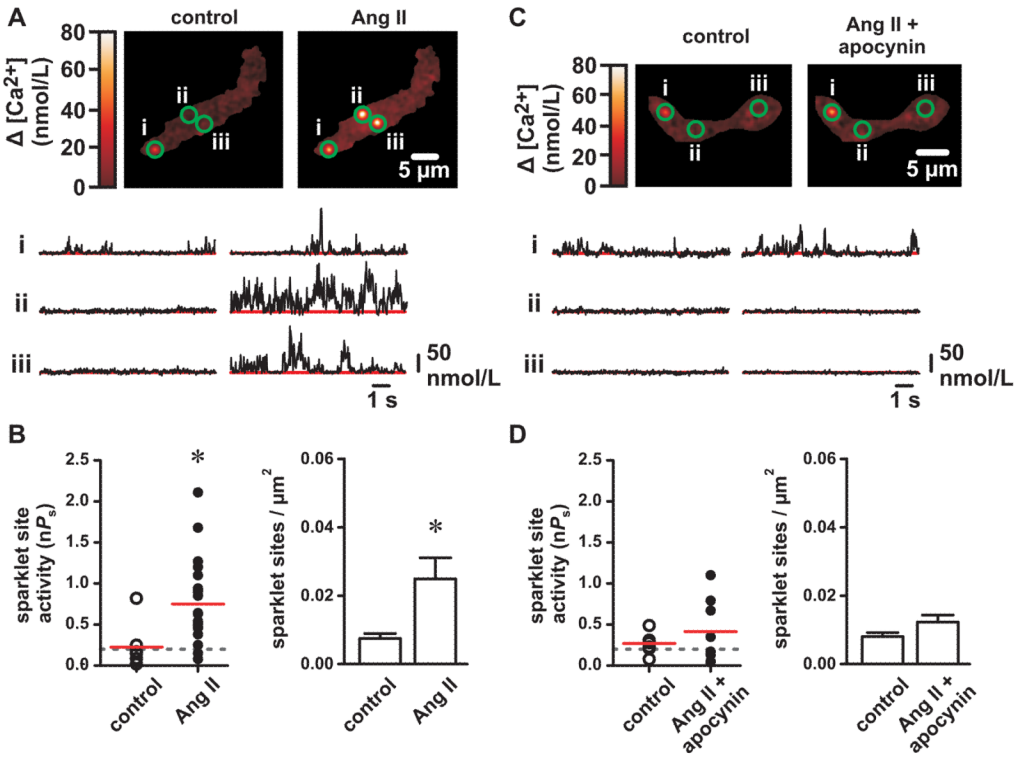

Figure 4. Inhibition of NADPH oxidase with apocynin prevents angiotensin II-dependent stimulation of L-type Ca^{2+} channel sparklet activity

A, Representative TIRF images showing Ca^{2+} influx in an arterial myocyte before and after application of angiotensin II (Ang II; 100 nmol/L). Traces show the time course of Ca^{2+} influx at the three circled sites. B, Plot of Ca^{2+} sparklet site activities (nP_s) and plot of mean ± SEM Ca^{2+} sparklet density (Ca^{2+} sparklet sites/μm^2) before and after Ang II (n=8 cells). C, Representative TIRF images show Ca^{2+} influx in an arterial myocyte before and after application of Ang II (100 nmol/L) in the presence of the NADPH oxidase inhibitor apocynin (25 μmol/L). Traces showing the time course of Ca^{2+} influx at the three circled sites. D, Plot of Ca^{2+} sparklet site activities (nP_s) and plot of mean ± SEM Ca^{2+} sparklet density (Ca^{2+} sparklet sites/μm^2) before after Ang II in the presence of apocynin (n=6 cells). *P<0.05

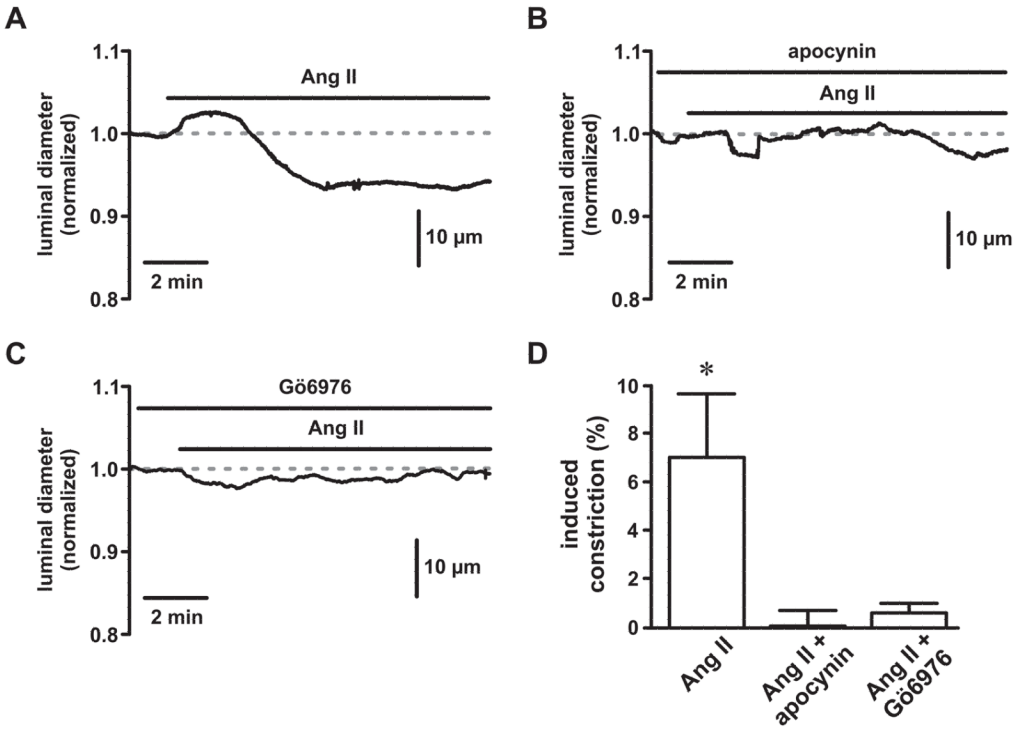

Figure 5. Inhibition of NADPH oxidase and PKC prevents angiotensin II-dependent constriction of cerebral arteries

A, B, & C, Representative time courses showing luminal diameters of pressurized (80 mm Hg) cerebral arteries exposed to angiotensin II (Ang II; 1 nmol/L) in the absence (panel A) or presence of the NADPH oxidase inhibitor apocynin (25 µmol/L; panel B) and the PKC inhibitor Gö6976 (100 nmol/L; panel C). D, Plot of the mean ± SEM induced constriction (%) by Ang II in the absence or presence of apocynin and Gö6976 (n=3 arteries). *P<0.05

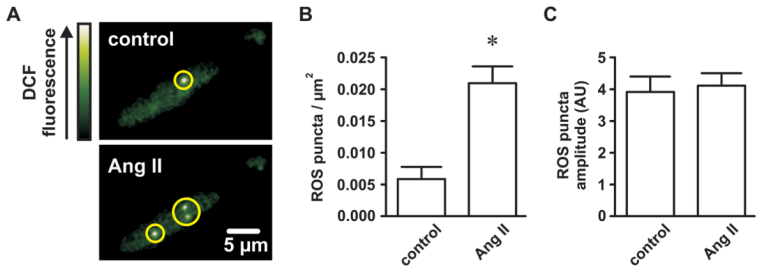

Figure 6. Angiotensin II promotes spatially restricted generation of reactive oxygen species in isolated cerebral arterial smooth muscle cells

A, Representative TIRF images showing punctate elevations of dichlorofluorescein (DCF) fluorescence (indicating reactive oxygen species formation) in an arterial myocyte before and after application of Ang II (100 nmol/L). B, Plot of the mean ± SEM reactive oxygen species (ROS) puncta density (ROS puncta/μm^2) before and after Ang II (n=6 cells). C, Plot of the mean ± SEM ROS puncta amplitude (arbitrary units; AU) before and after Ang II (n=6 cells). *P<0.05

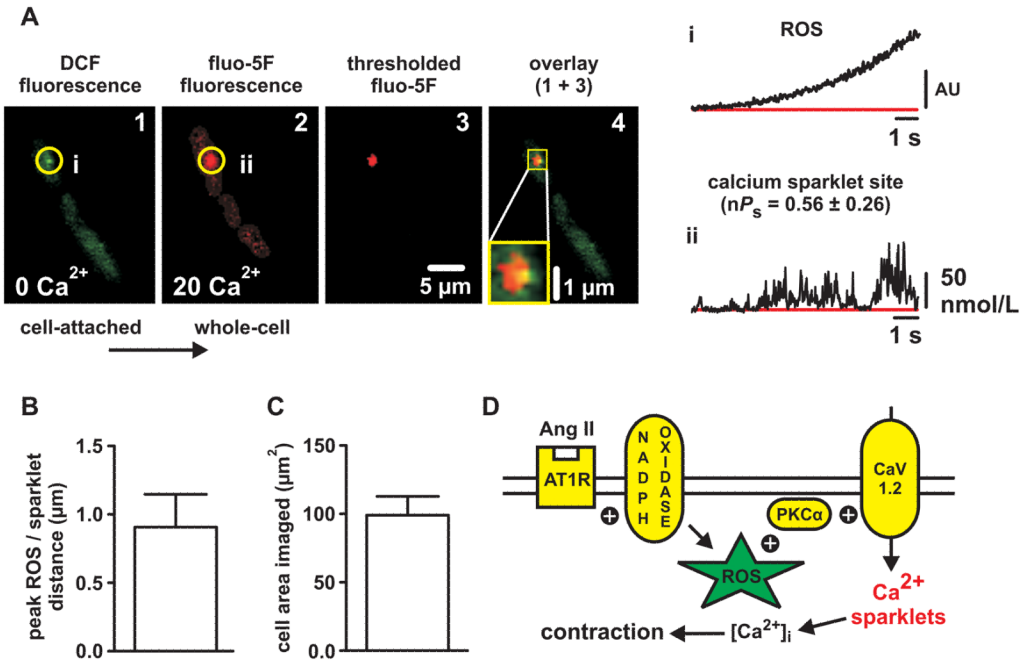

Figure 7. Local sites of elevated reactive oxygen species generation precede and colocalize with Ca^{2+} sparklet activity in cerebral arterial smooth muscle cells

A, Representative TIRF images of an arterial myocyte exposed to Ang II showing sequential DCF fluorescence (indicating ROS formation; panel 1) and fluo-5F fluorescence (indicating Ca^{2+} influx; panel 2). DCF fluorescence was obtained in Ca^{2+}-free solution prior to cell rupture and dialysis with fluo-5F and subsequent introduction of Ca^{2+} (20 mmol/L). Panel 4 shows an overlay of fluo-5F fluorescence thresholded to isolate Ca^{2+} sparklet activity (red; panel 3) with the DCF fluorescence (green; panel 1) to demonstrate colocalization (yellow) of punctate ROS generation and Ca^{2+} sparklet activity. Traces showing the time course of DCF fluorescence (i.e. ROS generation) at the site circled in panel 1 (i) and the time course of fluo-5F fluorescence (i.e. Ca^{2+} influx) at the site circled in panel 2 (ii). B, Plot of the mean ± SEM distance (in µm) between the peaks of ROS puncta and adjacent Ca^{2+} sparklet sites (n=6 ROS/Ca^{2+} sparklet sites from 5 cells). C, plot of the mean ± SEM cell area imaged (in μm^2) during the DCF/fluo-5F experiments (n=5 cells). D, Proposed mechanism by which local generation of ROS stimulate PKC-dependent L-type Ca^{2+} channel sparklet activity in cerebral arterial smooth muscle cells (see Discussion).